CHAPTER 1

CHAPTER 1

Physico-Chemical Studies on Microemulsion: Effect of Cosurfactant Chain Length on the Phase Behavior, Formation Dynamics, Structural Parameters and Viscosity of Water/(Tween 20+n-Alkanol)/n-Heptane Water-in-Oil Microemulsion

Abstract

The pseudo-ternary water-in-oil microemulsion system, comprising of water/(polyoxyethylene sorbitan monolaurate [Tween 20]+n-alkanol)/n-heptane, have been studied by phase manifestation, method of dilution, viscosity and dynamic light scattering measurements. Tween 20, in combination with equal mass of cosurfactants (of varying chain length, from n-butanol to n-octanol) were used in studying the systems in the temperature range 303 – 323 K. Appearance of turbidity was noted visually, which indicated the attainment of immiscibility or phase separation; a clear dependency of the different phases on cosurfactant chain length was noted. By employing the method of dilution, associated thermodynamic parameters for the formation of water-in-oil microemulsion droplets were derived. Different associated structural parameters were derived through further computation of the data derived from the method of dilution. Unusual behavior of Tween 20, compared to the conventional ionic surfactants, was noted. Viscosity measurements, as carried out at different composition and temperature, revealed the temperature and water pool size dependency of the microemulsion systems. Viscosity data did not follow the same trend during heating and the cooling process, due to condensation effect. This phenomenon was further confirmed by dynamic light scattering measurements.

J. Surfact. Deterg. **2011,** 14, 473-486

1. Introduction

Microemulsions (μEs) are thermodynamically stable isotropic dispersions of water-in-oil (w/o) or vice versa (o/w), stabilized by a surfactant monolayer[34,217]. The surfactant monolayer not only prohibits the direct contact between water and oil, but also reduces the interfacial tension between the two immiscible liquids. Beside water-in-oil or oil-in-water microemulsion, another type, like bi-continuous one is also possible. Type of microemulsion basically depends on the relative abundance of the two immiscible liquids[218]. Further details on the type and structure of microemulsion could be found in literature[30,219] and review[34]. Judicious mixing water, amphiphile and oil could spontaneously form a stable microemulsion. Thermodynamic stability, solubilizing capacity, optical transparency and isotropicity, etc., are some specific properties for which microemulsions find manifold applications in separation technology, food processing, cosmetics, drug encapsulations and nanoparticle synthesis, etc.[218] Besides, such compartmentalized entities could mimic biological systems too. Such applications of microemulsions have encouraged researchers around the globe in investigating different types of microemulsions. As there is no end in good science, research outcome in the field of microemulsions are considered to be fragmentary in nature.

A water-in-oil microemulsion is topologically similar to a reverse micelle[220]. When small amount of water is added to surfactant solution in oil, droplets of water get delineated from the non-polar phase. The delineation becomes possible due to the formation of a well-defined boundary by surfactant monolayer [221]. In most of the cases when single tailed surfactants are used as emulsifying agent, a fourth component becomes essential to maintain the curvature of the microemulsion droplets. Although small chain alkyl halides and amines could be used as the fourth component (known as cosurfactant) the most widely used cosurfactants are short chain n-alkanols[34]. Extensive research works have been done extensive works in studying the effect of n-alkanols as an additional stabilizer; still variations in different physico-chemical parameter such as the role of cosurfactant chain length are not so common in literature. Most commonly used cosurfactants include n-butanol, n-pentenol and n-hexanol for their better stabilizing efficiency in

microemulsion formation. However the exact reason on the better efficacy of these alkanols over the higher analogues are still not exactly known. Except a few cases studies on microemulsion using a series of n-alkanol are not available in the literature to the best of our knowledge[97,108,222-224]. This has motivated us in endeavoring the investigation on the water-in-oil microemulsion comprising of water/(Tween 20+n-alkanol)/n-heptane where the cosurfactant (n-alkanol) chain lengths were varied from n-butanol to n-octanol.

In this paper we have explored the effect of cosurfactant chain length on different physico-chemical parameters of w/o microemulsion as mentioned above. Cosurfactant chain length was varied from n-butanol to n-octanol. Also investigation on the physico-chemical properties of microemulsions have been carried out at different temperatures and different [water] / [Tween 20] mole ratio, ω. Above mentioned systems have been investigated by way of phase manifestation, method of dilution, viscosity and dynamic light scattering measurement. Such studies are believed to provide information on microemulsion in form of their formulation, energetics, and structural parameters.

2. Experimental

2.1. Materials

The non-ionic surfactant Tween 20 was purchased from Fluka, Switzerland. The cosurfactants n-butanol, n-pentanol, n-hexanol, n-heptanol and n-octanol were products from Lancster, England. All the materials were stated to be more than 99.5% pure and were used as received. HPLC grade n-heptane was obtained from E. Merck, Germany. Double distilled water was used throughout the experiment.

2.2. Methods

2.2.1. Construction of the phase diagram.

The pseudo ternary phase diagram comprising of water/(Tween 20+n-alkanol)/n-heptane was constructed by the method of titration and through visual inspection [211]. To investigate different regions (mainly two phase turbid,

2Φ and homogeneous single phase, 1Φ), known amount of Tween 20, mixed with n-alkanol in 1:1 ratio (w/w) were taken in different stoppered test tubes. Varying amount of oil (or water) was then added. Water (or oil) was progressively added by using Hamilton (USA) microsyringe under constant stirring condition where the temperature was controlled using a cryogenic circulatory water bath (of precession ±0.1K) at 303K. Appearance of the state of turbidity was noted visually, which indicated the onset of phase separation or immiscibility. The solutions were allowed to attain equilibrium for 30 minutes (we found that equilibrium was attained within thistime period in most of the systems).The process was followed for all the cosurfactants (n-butanol to n-octanol) [225].

2.2.2. Method of dilution

Thermodynamics of formation of water-in-oil (w/o) microemulsion (μE) comprising water/(Tween 20+n-alkanol)/n-heptane were evaluated by the method of dilution. In this method, besides using a series of alkanols, experiments were carried out at different [water] / [Tween 20] mole ratio, ω (5, 10, 15 and 20) and at five different temperatures (303, 308, 313, 318 and 323K). Temperature was controlled by a cryogenic circulatory water bath with an accuracy of ±0.1K. The method of dilution also helped in evaluating different structural parameters of the microemulsion under various conditions. Briefly, in the method of dilution, a fixed amount of water, surfactant and oil were taken in a stoppered test tube. The turbid solution was then titrated with cosurfactant under constant stirring unless a clear solution appeared. Sufficient time was allowed in attaining the equilibrium. At this point of clarity, composition of the mixture was then noted. A known quantity of n-heptane was then further added whereby the microemulsion got destabilized[12]. Clarity of the microemulsion was regained by further addition of n-alkanol under constant stirring; the amount of cosurfactant required was again noted. This method of destabilization and re-stabilization was repeated to obtain several points. Experiments were then done under different conditions, viz., [water]/[Tween 20] mole ratio, ω, temperature and cosurfactant chain length in order to evaluate thermodynamic and structural parameters. Each set of

experiment was carried out at least four times and the average of the values were used in obtaining the final result [226].

2.2.3. Viscosity measurements

Viscosity measurements were performed on monophasic microemulsions of known composition where 0.2 moldm^{-3} Tween 20 in n-heptane, mixed with 1:1 (w/w) alkanols were used. Choice of such composition was intended for comparative studies. Solutions of different ω were then used for viscosity measurements using a LVDV-II+PCP cone and plate type roto viscometer (Brookfield Eng. Lab, USA). A CPE-42 type spindle made by Brookfield Eng. Lab, USA was used. Viscosity of microemulsion at different temperature was measured where the temperature was controlled by circulatory water bath (±0.1K). Microemulsion comprising n-octanol as cosurfactant, at ω=20 could not be studied at 0.2 moldm^{-3} Tween 20 as the solution appeared turbid. During the measurement shear rates (D) were varied within the range 20 – 60 S^{-1} and corresponding shear stress (τ) were recorded. Finally viscosity of a solution was obtained using the zero shear rates according to the relation $\eta = \tau / D$ [114,127,128].

2.2.4. Dynamic light scattering (DLS) studies

Solutions, as prepared in the viscosity measurements, were used in measuring the dimension of the microemulsion droplets by dynamic light scattering method under different set of conditions (viz., cosurfactant chain length, ω and temperature). Diameter of the microemulsion droplets were determined using a Zetasizer Nano ZS90 (ZEN3690, Malvern Instruments Ltd, U.K.). A He-Ne laser of 632.8 nm wavelength was used and the measurements were made at a scattering angle of 90^0. Temperature was controlled by inbuilt Peltier heating-cooling device (±0.05K). Refractive index of each solution was recorded with an ABBE type refractometer, as it was required as an input in determining the size of the μE droplet by DLS technique. Viscosity data, as obtained from viscosity measurements, were also used in processing DLS data. Samples were filtered thrice using Milipore™ hydrophobic membrane filter of 0.25μ pore size. In actual DLS measurements,

the diffusion coefficient (D) of a solution is measured which is related to the diameter of a droplet (d) according to Stokes–Einstein equation [133-137]:

$$D = \frac{kT}{3\pi\eta d} \qquad \textbf{(1.1)}$$

where k, T and η indicate the Boltzman constant, temperature and viscosity respectively.

3. Results and discussion

3.1. Phase manifestation

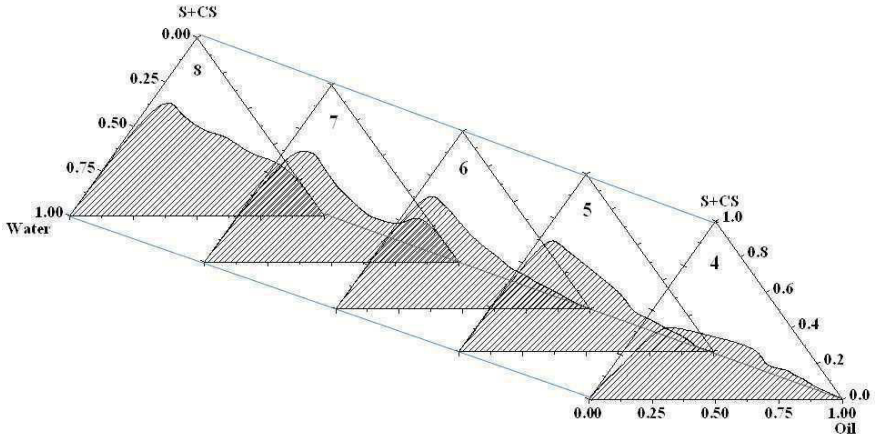

Figure 1.1. Pseudo-ternary phase diagram of water/(Tween 20 +n-alkanol)/n-heptane system at 303K. Tween 20 and n-alkanol were taken in 1:1 w/w ratio. n-alkanol chain lengths are mentioned inside each plot. Scale magnitudes were reduced by 1/100 in the plot.

Figure 1.1 describes the pseudo ternary phase diagram of water/(Tween 20+n-alkanol)/n-heptane systems. Solid line indicates the boundary region between the clear, single phase (1Φ) microemulsion region (un-shaded portions in the Figure) and two phase (2Φ) turbid region (shaded portions). From the Figure 1.1 it is also noticeable that the area under the clear region was dependent on the cosurfactant chain length. Results have further been clarified through Figure 1.2. With the increase in cosurfactant chain length, area under the monophasic region decreased with a small halt at n-hexanol. Area under the monophasic region was ~55 % (n-butanol) which decreased progressively upto ~25 % in case of n-octanol. n-pentanol and n-hexanol tendered more or less similar effects. It could be concluded, therefore, that increase in cosurfactant chain length (decrease in polarity) makes the

homogeneous system unstable, i.e., clear microemulsion formation becomes less favorable with the increasing cosurfactant (n-alkanol) chain length. Although different regions (viz., gel, viscous and clear fluid) were recorded in the monophasic region, for a simple and better understanding on the effect of n-alkanol chain length results have been described in terms of only two phases (1Φ and 2Φ).

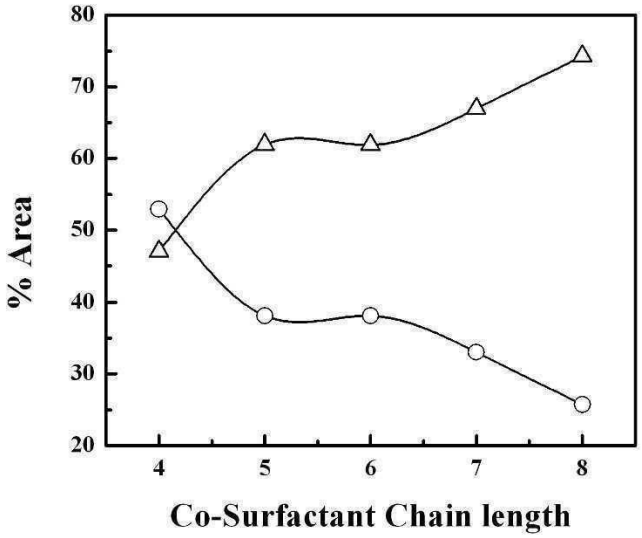

Figure 1.2. *Interdependence of the % area under clear (O) and turbid (Δ) region* with the cosurfactant chain length for water/(Tween 20 +n-alkanol)/n-heptane pseudo-ternary system at 303 K.

Construction of the phase diagram is the first and foremost job to be executed by a researcher, although the process is tedious in nature [34]. It is known that the phase behavior of pseudo-ternary system depends on various factors, viz., nature of the polar medium (herein water), surfactant and cosurfactant used, presence of additive, nature of the nonpolar medium (oil, herein n-heptane) and temperature, pressure, etc. [34,92] According to Ninham et al. the compactness/ease of microemulsion formation depends on the packing symmetry between the surfactant chain length and the combined chain length of oil and used cosurfactant [227]. Tween 20 has a hydrocarbon tail comprising of 12 carbon atoms. It is, therefore, not unexpected that n-pentanol and n-hexanol would have a matching symmetry when combined with n-heptane. Appearance of larger monophasic region in case of n-butanol could be explained by its higher miscibility with water[223]. Higher n-alkanols ($>C_6$) behaved more like oil than cosurfactant.

3.2. Dilution method

3.2.1. Evaluation of thermodynamic parameters

For a stable μE, the alkanol is distributed in water, interface and oil; the surfactant essentially remains at the interface. The total number of moles of n-alkanol (n_a^i) would thus follow the relation:

$$n_a^t = n_a^w + n_a^i + n_a^o \quad \textbf{(1.2)}$$

where the superscripts w, i and o stand for water, interface and oil respectively.

At a constant temperature and fixed ω, the ratio of number of moles of alkanol to the number of moles of alkanol in oil (n_a^o) will be constant (with respect to the total number of it in the oil, n_o). Consequently, the mole fraction ratio of alkanol at the interface (X_a^i) and in oil (X_a^o) should also be constant. Thus,

$$n_a^o/n_o = k \quad \textbf{(1.3)}$$

and $$\frac{X_a^i}{X_a^o} = k_d \quad \textbf{(1.4)}$$

where, k and k_d are constant and the distribution constant respectively.

By replacing equation (1.3) in equation (1.2) one sets the following relation:

$$\frac{n_a^t}{n_s} = \frac{n_a^w + n_a^i}{n_s} + k\frac{n_o}{n_s} \quad \textbf{(1.5)}$$

n_s represents the number of moles of surfactant.

In the dilution experiment, at a fixed n_s, n_a^t and n_o are varied to have a series of $\frac{n_a^t}{n_s}$ and $\frac{n_o}{n_s}$ which according to equation (1.5) can give $\frac{n_a^w + n_a^i}{n_s}$ and k

from the linear plot between $\frac{n_a^t}{n_s}$ and $\frac{n_o}{n_s}$ as intercept (I) and slope (S) respectively. For n-butanol, which is a lower alkanol, n_a^w can be obtained from its water solubility, and by this value $\frac{n_a^i}{n_s}$ can be evaluated. Higher n-alkanols are practically insoluble in water; thus $\frac{n_a^i}{n_s}$ could directly be obtained from the intercept. The plot of $\frac{n_a^t}{n_s}$ vs $\frac{n_o}{n_s}$ for n-hexanol at ω=10 have been presented in Figure 1.3. The distribution constant k_d is related to the slope and intercept of equation (1.5) as:

$$k_d = \frac{X_a^i}{X_a^o} = \frac{n_a^i/(n_a^i + n_s)}{n_a^o/(n_a^o + n_o)} = \frac{n_a^i(1+\frac{n_a^o}{n_o})}{n_a^o(n_a^i + n_s)} \qquad \textbf{(1.6)}$$

Alternately,

$$k_d = \frac{\alpha(1+S)}{S[1+(I-\frac{n_a^w}{n_s})]} = \frac{\alpha(1+S)}{S(1+\alpha)} \qquad \textbf{(1.7)}$$

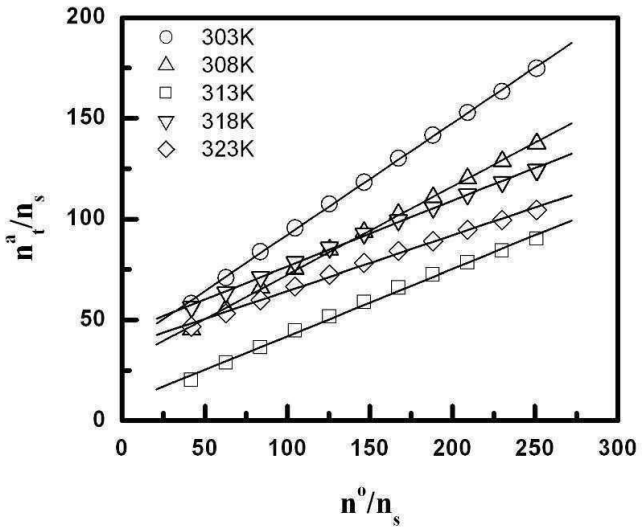

Figure 1.3. Plot of n_a^t/n_s vs n_o/n_s for water/(Tween 20 +n-hexanol)/heptane water-in-oil microemulsion system. A 1:1 (w/w) mixture of Tween 20 and n-hexanol was used at [water]/[Tween 20] mole ratio, ω=10. Temperatures are mentioned inside the Figure.

where, $$\alpha = (I - \frac{n_a^{\,w}}{n_s}) = \frac{n_a^{\,i}}{n_s} \qquad (1.8)$$

Therefore, by knowing I, S and α, one can obtain the value of k_d. For alkanols larger than n-butanol α =I, and equation (1.7) could be approximated as;

$$k_d = \frac{I(1+S)}{S(1+I)} \qquad (1.9)$$

Thus by using equations 1.5, 1.7 and 1.9 one can evaluate the values of $n_a^{\,i}$, $n_a^{\,o}$ and k_d which are useful information for the formation of w/o microemulsion. Evaluation of k_d value is required in obtaining the information on the thermodynamics of the involved process.

Changes in the standard Gibbs free energy of transfer (ΔG_t^o) of alkanol from oil to the interface could be expressed as:

$$\Delta G_t^o = - RT \ln k_d \qquad (1.10)$$

Changes in the standard enthalpy of transfer ΔH_t^o was evaluated by the van't Hoff equation:

$$[\frac{\partial(\Delta G_t^{\,o})}{\partial(1/T)}]_p = \Delta H_t^{\,o} \qquad (1.11)$$

In the present study, ΔG_t^o vs. T profile was found to follow a 2^0 polynomial equation as:

$$\Delta G_t^o = a + bT + cT^2 \qquad (1.12)$$

where a, b and c are the polynomial coefficients.

The polynomial coefficients thus helped in determining the ΔH_t^o values described in the following expression:

$$[\frac{d(\Delta G_t^{\,o}/T)}{d(1/T)}]_p = a - cT^2 = \Delta H_t^{\,o} \qquad (1.13)$$

The standard entropy of transfer (ΔS_t^o) of the associated process was then evaluated according to the following expression:

$$\Delta S_t^o = (\Delta H_t^o - \Delta G_t^o)/ T \qquad (1.14)$$

Figure 4 describes the variation of ΔG_t^o with [water]/[Tween 20] mole ratio (ω) at different temperature for water/(Tween 20+n-hexanol)/n-heptane as representative.

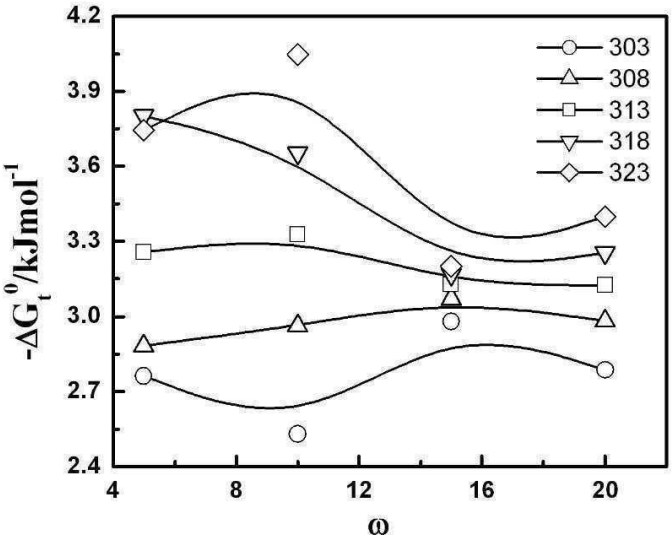

Figure 1.4. *ΔG_t^0 vs. ω plot* for water/(Tween 20 +n-hexanol, 1:1,w/w)/n-heptane water-in-*oil microemulsion at ω=10. Temperatures (in K) are mentioned inside the* Figure.

Results are also summarized in Tables 1.1 to 1.5.

Table 1.1. Thermodynamic parameters for the transfer of n-hexanol from oil to oil-water interface in the formation of water/(Tween 20+n-hexanol)/n-heptane water-in-oil microemulsion at different temperature and [water]/[Tween 20*] mole ratio, ω.*

Parameter		Temp. / K				
	ω	303	308	313	318	323
k_d	5	2.99	3.08	3.40	4.21	4.03
	10	2.73	3.18	3.59	3.98	4.51
	15	3.26	2.97	3.32	3.13	3.29
	20	3.09	2.82	2.47	2.65	3.54
$(-)\Delta G^0_t$/kJmol^{-1}	5	2.76	2.88	3.25	3.80	3.74
	10	2.53	2.96	3.32	3.65	4.04
	15	2.98	3.07	3.13	3.16	3.20
	20	2.80	2.98	3.12	3.25	3.39
ΔH^0_t /kJmol^{-1}	5	17.99	16.40	14.71	13.03	11.32
	10	22.00	21.00	19.98	18.94	17.90
	15	2.48	1.36	0.23	-0.92	-2.09
	20	8.15	7.20	6.23	5.24	4.25
ΔS^0_t/JK^{-1}mol^{-1}	5	68.51	62.51	57.41	52.93	46.64
	10	81.00	77.81	74.50	71.10	67.94
	15	18.04	14.40	10.73	7.06	3.42
	20	36.12	33.07	29.90	26.73	23.67

Table 1.2. Thermodynamic parameters for the transfer of n-alkanol from oil to oil-water interface in the formation of water/(Tween 20+n-alkanol)/n-heptane water-in-oil microemulsion at 313K and at different and [water]/[Tween 20] *mole ratio, ω.*

n-alkanol	Parameter				
	ω	k_d	$(-)\Delta G^0_t$ /kJmol^{-1}	ΔH^0_t /kJmol^{-1}	ΔS^0_t/JK^{-1}mol^{-1}
BuOH	5	3.01	2.86	27.42	96.75
	10	2.84	2.71	12.26	47.87
	15	2.38	2.08	11.56	0.043
	20	1.94	1.72	11.34	41.76
PentOH	5	3.41	3.19	13.41	53.05
	10	2.94	2.81	8.83	37.22
	15	2.60	2.50	-0.86	5.18
	20	2.47	2.35	4.30	21.29
HexOH	5	3.49	3.25	14.71	57.41
	10	3.59	3.32	19.99	74.50
	15	3.32	3.13	0.23	10.73
	20	2.47	3.12	6.23	29.90
HeptOH	5	3.52	3.43	7.67	35.47
	10	3.57	3.31	12.10	49.24
	15	3.30	3.39	6.18	30.59
	20	3.00	3.11	4.50	24.24
OctOH	5	4.34	3.82	11.76	49.78
	10	4.09	3.62	8.64	39.21
	15	3.48	3.24	2.27	17.62
	20	2.69	3.05	15.04	57.82

Table: 1.3. Free energy change ($-\Delta G^0_t$) for the transfer of n-alkanol from oil to oil-water interface in the formation of water/(Tween 20+n-alkanol)/n-heptane water-in-oil microemulsion at different temperatures and [water]/[Tween 20*] mole ratio, ω.*

System	$-\Delta G^0_t$ values at different temperatures					
	ω	**303**	**308**	**313**	**318**	**323**
BuOH	5	1.21	2.30	2.86	3.00	3.09
	10	2.23	2.31	2.71	2.84	3.16
	15	1.55	1.62	2.25	2.17	2.35
	20	1.49	1.65	1.72	2.30	2.22
PentOH	5	2.65	2.83	3.19	3.41	3.69
	10	2.54	2.79	2.81	3.17	3.29
	15	2.86	3.10	2.48	3.08	2.99
	20	2.16	2.25	2.35	2.50	2.56
HexOH	5	2.76	2.88	3.25	3.80	3.74
	10	2.53	2.96	3.32	3.65	4.04
	15	2.98	3.07	3.13	3.16	3.20
	20	2.78	2.98	3.12	3.25	3.39
HeptOH	5	3.09	3.26	3.43	3.60	3.80
	10	2.67	2.94	3.31	3.42	3.63
	15	3.01	3.21	3.39	3.53	3.61
	20	2.79	2.96	3.11	3.21	3.28
OctOH	5	3.04	3.68	3.82	3.75	4.28
	10	2.74	3.20	3.62	3.81	3.44
	15	2.89	3.11	3.24	3.27	3.29
	20	2.08	2.73	3.05	3.21	3.28

Table: 1.4. Enthalpy change ($-\Delta H^0_t$) for the transfer of n-alkanol from oil to oil-water interface in the formation of water/(Tween 20+n-alkanol)/n-heptane water-in-oil microemulsion at different temperatures and [water]/[Tween 20*] mole ratio, ω.*

System	ΔH^0_t values at different temperatures				
	ω	**303**	**308**	**313**	**318**	**323**
BuOH	5	67.48	46.36	24.91	3.11	-19.03
	10	8.85	10.56	12.30	14.06	15.85
	15	20.53	16.07	11.53	6.93	2.25
	20	11.23	11.29	11.34	11.40	11.45
PentOH	5	12.60	13.00	13.41	13.82	14.25
	10	7.40	8.12	8.83	9.56	10.30
	15	-10.28	-5.61	-0.86	3.96	8.86
	20	4.57	4.44	4.30	4.16	4.02
HexOH	5	17.99	16.36	14.71	13.03	11.32
	10	22.01	21.00	19.99	18.94	17.90
	15	2.48	1.37	0.23	-0.92	-2.09
	20	8.15	7.20	6.23	5.24	4.24
HeptOH	5	6.61	7.13	7.67	8.20	8.75
	10	18.99	15.58	12.10	8.56	4.98
	15	10.95	8.60	6.18	3.74	1.25
	20	8.79	6.65	4.48	2.26	0.02
OctOH	5	19.45	15.64	11.76	7.81	3.81
	10	42.03	25.48	8.64	-8.45	-25.82
	15	11.26	6.80	2.27	-2.33	-7.01
	20	38.50	26.86	15.04	3.01	-9.20

Table: 1.5. Entropy change ($-\Delta S^0_t$) for the transfer of n-alkanol from oil to oil-water interface in the formation of water/(Tween 20+n-alkanol)/n-heptane water-in-oil microemulsion at different temperatures and [Water]/[Tween 20*] mole ratio, ω.*

System	ΔS^0_t values at different temperatures					
	ω	**303**	**308**	**313**	**318**	**323**
BuOH	5	226.72	158.02	88.75	19.22	-49.33
	10	36.59	41.80	47.96	53.2	58.87
	15	72.90	57.40	44.06	28.64	14.24
	20	42.00	42.02	41.76	43.09	42.34
PentOH	5	50.33	51.41	53.05	54.22	55.54
	10	32.85	35.42	37.22	40.06	42.11
	15	-24.52	-8.14	5.18	22.15	36.71
	20	22.24	21.73	21.29	20.98	20.40
HexOH	5	68.51	62.51	57.41	52.93	46.64
	10	81.00	77.81	74.50	71.10	67.94
	15	18.04	14.40	10.73	7.06	3.42
	20	36.12	33.07	29.90	26.73	23.67
HeptOH	5	32.04	33.76	35.47	37.13	38.88
	10	71.49	60.15	49.24	37.70	26.67
	15	46.10	38.31	30.59	22.9	15.08
	20	38.25	31.23	24.24	17.24	10.23
OctOH	5	74.27	62.74	49.78	36.4	25.04
	10	147.8	93.13	39.21	-14.58	-69.29

System	ΔS^0_t values at different temperatures				
	ω	**303**	**308**	**313**	**318**	**323**
	15	46.72	32.20	17.62	2.96	-11.52
	20	133.95	96.12	57.82	19.59	-18.31

ΔG_t^o values were found to be negative in all the cases, which indicate the spontaneity of microemulsion formation. Tween 20, along with n-alkanol, can tune the curvature of the water droplets, delineated from the contact of oil. It is clear from the results that with the rise in temperature for a particular alkanol, the negative value of ΔG_t^o increased. Higher negativity of ΔG_t^o represents enhanced spontaneity of the microemulsion formation process. Increase in temperature would lead to the overall increase in the kinetic energy of the system, which subsequently eases the easier formation of droplet. Increase in temperature might lead to the opening up of the coiled surfactant head group, for which better efficacy of the system could have been achieved by Tween 20 at higher temperature [226].

A decrease in the negative value of ΔG_t^o with increasing [water]/[Tween 20] mole ratio ω was observed in general. Increase in the volume of the water droplet with increasing ω value requires larger coverage or delineation of water from the hydrophobic environment. At a fixed surfactant/cosurfactant composition, thus spontaneity of the microemulsion formation would be limited with the progressive increase in ω values.

While considering the effect of cosurfactant chain length, the spontaneity of the process is increased with the increase in cosurfactant chain length. However, no significant difference was noticed between n-heptanol and n-octanol. Increase in cosurfactant chain length leads to better accommodation of n-alkanol at the oil-water interface. However, the alkanols larger than n-heptanol behaved more like oil than cosurfactant. Overall values of ΔG_t^o were found to be within the range of -1 to -5 $kJ\,mol^{-1}$. The lower ΔG_t^o are indicative of weak interactions between the alkanol and Tween 20 at the interface [223].

While considering the ΔH_t^o value under various conditions (as described in Tables 1.1-1.2 and Table 4) it was found that, except a few case, the ΔH_t^o values were positive. Positive ΔH_t^o values indicate endothermicity involved in the microemulsion formation process. This was as expected; while water droplets getting dispersed into the oil continuum, due to area enhancement, there would be absorption of heat (energy). In general ΔH_t^o values decreased with the rise in ω value. It also decreased with the increase in temperature. With the rise in temperature overall structuredness of the system decreases, thus energy change associated with the process gets decreased. However, ΔH_t^o values were found to decrease with the increasing n-alkanol chain length. With the increase in n-alkanol chain length, partitioning of the cosurfactant at the oil-water interface becomes easier. Entropy values were found to be positive in most of the cases. Variation in the ΔS_t^o value was not so significant compared the associated enthalpy changes. ΔS_t^o values decreased with the rise in ω values; however, ΔS_t^o values increased linearly with the rise in cosurfactant chain length.

Investigation on the enthalpy entropy compensation could justify the similarities in the structuredness of a reverse micelle and water-in-oil microemulsion system. Normally the compensation effect is stated to be valid for surfactant aggregates [101]. Plot of ΔH_t^o vs ΔS_t^o have been shown in Figure 1.5. In this plot all the compositions/conditions were taken into account except n-butanol. Microemulsion system comprising n-butanol behaved differently for its significant solubility in water compared to its higher homologs 140. Nice correlation was observed for all sets of values (different n-alkanols, ω values and temperature). Compensation temperature, as obtained from the slope, was found to be 314K which was in good agreement with the average all the experimental temperature range (average temperature: 313K; experimental temperature range: 303, 308, 313, 318 and 323K). Although the energetic parameters have been indirectly computed, however they could also be experimentally evaluated by calorimetric measurements. Such studies could be considered as one of the future perspective.

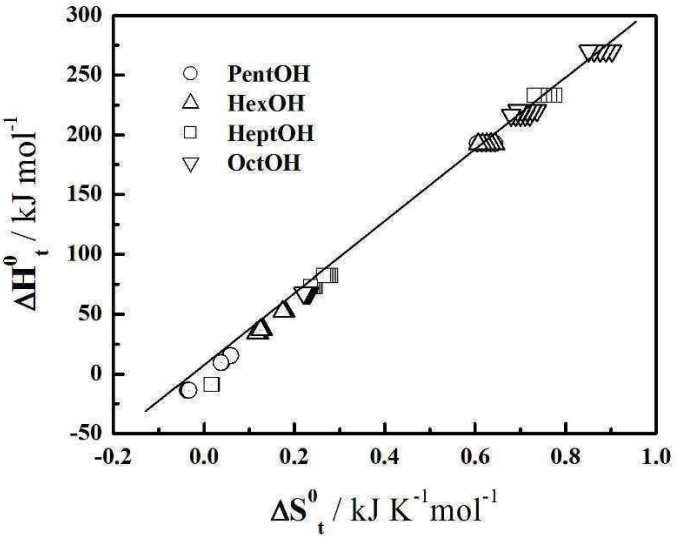

Figure 1.5. Enthalpy-entropy compensation for the formation of water/(Tween 20 + n-alkanol)/n-heptane water-in-oil microemulsion (except n-butanol as it followed *different path). All the ω values at different experimental temperature were* considered. n-alkanols used have been mentioned inside the Figure. Compensation temperature: 314K (close to the average of the experimental temperature range 303-323K, i.e., 313K).

3.2.2. Structural parameters

The results of dilution experiments could suitably be further computed in evaluating different structural parameters of the w/o microemulsion. The microemulsion droplets are approximated to have spherical shape in general, mono dispersed with a surface mono layer comprising surfactant and cosurfactant to be present at the interface. The total volume of the dispersed droplets (V_d) per unit volume (here in mL) can be expressed as follows:

$$V_d = \frac{4}{3}\pi R_e^{\,3} N_d \qquad (1.\mathbf{15})$$

R_e and N_d represents the effective diameter and total number of the droplets respectively.

The droplet surface area (A_d) of droplets per unit volume is therefore:

$$A_d = 4\pi R_e^{\,2} N_d = (n_S A_S + n_a^{\,i} A_a) N_A \qquad (1.\mathbf{16})$$

where, A_S and A_a are the cross sectional area of the surfactant and cosurfactant molecules respectively, N_A Avogadro's constant.

The equation for R_e from equation 1.15 and 1.16 can be written as:

$$R_e = 3V_d/A_d \qquad (1.17)$$

Total volume of the dispersed phase, herein the water droplet embedded by the surfactant and n-alkanols at the oil-water interface, is the sum of the volume contribution of water (V_{H_2O}), surfactant (V_S) and the interfacial n-alkanol molecules (V_a^i) at the interface respectively. Thus one could write;

$$V_d = V_{H_2O} + V_S + V_a^i \qquad (1.18)$$

One can determine the respective volumes using the values of number of moles (n_a^i), molar mass (M_a) and density of the components (ρ_a) according to the relation:

$$V_a^i = n_a^i M_a/\rho_a \qquad (1.19)$$

The total droplet surface area (A_d) can be obtained from the equation:

$$A_d = (n_S A_S + n_a^i A_a) N_A \qquad (1.20)$$

where, A_S and A_a are the polar head group area of surfactant and alkanol, respectively, and N_A is the Avogadro constant.

Putting the value of R_e in equation (1.15) we get the values of N_d

$$N_d = 3V_d/4\pi R_e^3 \qquad (1.21)$$

The average aggregation number of surfactant (N_S) and cosurfactant (N_a) in a microemulsion droplet can be expressed as:

$$N_S = \frac{n_S N_A}{N_d} \qquad (1.22)$$

$$N_a = \frac{n_o^i N_A}{N_d} \qquad (1.23)$$

Volume of a microemulsion droplet is contributed by dispersed water, surfactant and cosurfactant molecules. Thus the radius of water pool in a microemulsion droplet is related to the effective radius (i.e., the sum of pool radius and surfactant tail) according to the relation:

$$R_w = \left(\frac{V_{H_2O} + V_S{}^h + V_a{}^h}{V_d}\right)^{1/3} R_e \qquad (1.24)$$

where V_{H_2O} , $V_S{}^h$ and $V_a{}^h$ are volume of water droplet, surfactant head group, and alkanol head group, respectively. Volume contribution due to surfactant head group and cosurfactant head group could be evaluated from the following two equations:

$$V_S{}^h = \frac{4}{3\pi^{1/2}} A_S{}^{3/2} N_S \qquad (1.25)$$

$$V_a{}^h = \frac{4}{3\pi^{1/2}} A_a{}^{3/2} N_a \qquad (1.26)$$

Various structural parameters, as described in the earlier section were computed by employing the dilution data into the aforementioned equations. Variation in the number of droplets per unit volume (N_d) with [water]/[Tween 20] mole ratio and temperature is shown in Figure 6 for microemulsion comprising n-hexanol as representative. Detailed results for all the systems are also summarized in Table 1.6.

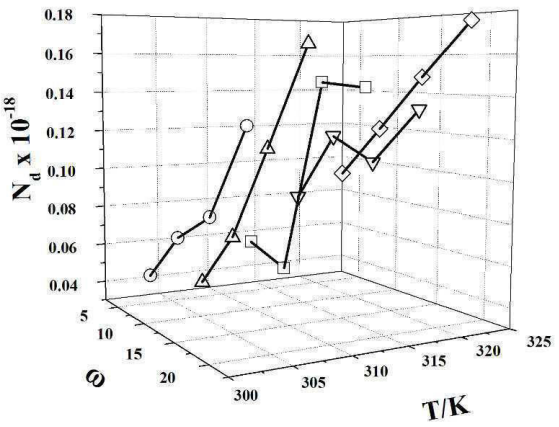

Figure 1.6. N_d - ω - T profile for water/(Tween 20 +n-hexanol)/n-heptane water-in-oil microemulsion system. A 1:1 (w/w) Tween 20: n-hexanol mixture was used.

Number of droplets per unit volume (herein mL) was found to increase with the increase in ω values. Such results apparently seem to be contradictory as one could expect an incremental effect when the volume of the added water is increased for a particular system at fixed surfactant/cosurfactant and oil and at a certain temperature.[223,228] This unusual behavior was only observed in our earlier investigations.[226,229] Such behavior was observed only for nonionic surfactants having polyoxyethylene head groups[230,231]. It is assumed that with the increase in the volume of water, newer droplets could be formed with smaller dimensions. This assumption would further be established by analyzing the other structural parameters as well as the dynamic light scattering measurements to be presented in subsequent sections. We also expect occurrence of droplet fission phenomena while the temperature of the microemulsion media were increased.

With the increase in the number of droplets through the progressive addition of water to a fixed amount of surfactant, alkanol and oil, if the number of droplet increases, one could also expect in the change of number of surfactant (N_s) and cosurfactant (N_{cs}) molecules per microemulsion droplet. ω and temperature dependence of N_s and N_{cs} for water/(Tween 20+n-hexanol)/n-heptane water-in-oil microemulsion system is shown in Figure 1.7 as representative.

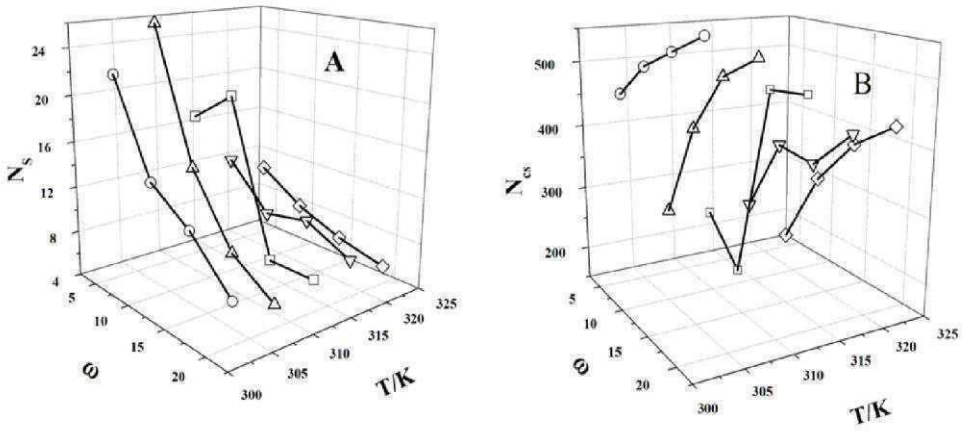

Figure 1.7. Variation in the number of A) surfactant (N_s) and B) cosurfactant (N_{cs}) per microemulsion droplet with ω and temperature in water/(Tween 20 +n-hexanol)/n-heptane water-in-oil microemulsion system.

Table 1.6. Structural parameters of Water/(Tween 20+n-alkanol)/n-Heptane water-in-oil microemulsion at at different temperatures and and [Water]/[Tween 20*] mole ratio, ω.*

n-alkanol		$10^{-18}N_d$(per mL)/N_s (per droplet)/ /N_{cs} (per droplet)				
	ω	**303**	**308**	**313**	**318**	**323**
BuOH	5	1.47/66.33/36.37	4.08/23.93/124.61	7.09/13.77/124.26	7.63/12.78/34.67	0.13/7.65/87.72
	10	2.06/47.22/186.22	3.96/24.64/154.12	5.50/17.73/101.92	8.15/11.96/90.33	0.11/8.66/83.52
	15	1.42/68.42/138.70	2.82/34.50/118.34	4.60/21.28/93.52	7.86/12.41/110.97	0.10/8.96/102.39
	20	3.43/28.38/324.36	8.97/10.87/289.03	6.55/14.90/188.84	7.76/12.60/134.29	8.83/11.05/78.45
PentOH	5	4.04/24.15/316.82	4.45/21.93/192.57	7.46/13.07/202.17	0.10/9.65/188.96	0.12/8.04/157.30
	10	6.78/14.38/396.03	8.39/11.64/336.23	9.08/10.75/271.30	0.11/8.57/243.52	0.13/7.44/208.30
	15	0.12/8.37/435.33	0.12/8.41/383.26	0.12/8.18/331.05	0.14/6.57/308.91	0.15/6.45/261.00
	20	0.12/8.49/447.06	0.15/6.64/409.31	0.17/5.75/378.31	0.16/5.87/336.19	0.19/5.17/312.85
HexOH	5	0.45/21.85/454.01	0.38/25.72/255.04	0.57/17.05/238.63	0.80/12.16/240.20	0.92/10.61/171.24
	10	0.70/13.87/509.71	0.68/14.30/411.56	0.49/19.78/172.17	0.12/8.34/366.92	0.12/8.13/300.20
	15	0.86/11.41/542.40	0.12/8.44/503.76	0.15/6.68/478.83	0.11/9.17/360.00	0.15/6.57/380.04
	20	0.13/7.56/574.27	0.16/5.97/542.21	0.14/6.75/488.09	0.13/7.28/426.23	0.18/5.54/428.05
HeptOH	5	3.33/29.33/470.23	3.96/24.66/326.04	5.76/16.96/324.30	6.68/14.62/223.63	8.48/11.51/227.21
	10	6.35/15.38/639.54	7.28/13.42/563.95	8.59/11.36/511.96	9.19/10.62/441.03	0.10/9.68/383.14
	15	7.58/12.87/679.39	9.36/10.43/628.14	0.10/9.34/577.10	0.12/8.31/536.52	0.11/9.02/435.22
	20	0.11/9.28/719.85	0.13/7.69/679.30	0.13/7.76/624.15	0.13/7.66/569.35	0.13/7.27/523.16
OctOH	5	8.47/11.53/298.14	8.57/11.39/232.62	0.11/9.04/193.72	0.14/6.93/174.43	0.16/6.28/136.21
	10	0.15/6.35/323.92	0.18/5.55/291.39	0.16/5.95/250.99	0.19/5.25/223.89	0.20/4.82/196.90
	15	0.19/5.16/333.74	0.23/4.20/307.76	0.25/3.96/283.84	0.26/3.77/260.98	0.24/4.02/228.36
	20	0.28/3.53/338.60	0.30/3.22/318.20	0.28/3.52/295.36	0.33/2.96/281.09	0.35/2.81/264.18

Results have also been detailed in Table 1.6. It is evident from the Figure and Table 1.6 that the N_s value decreased with the increase in the ω. N_s also decreased with the increase in temperature. Such behavior contradicts the earlier reports by Hait et. al where a water in oil microemulsion comprising of water/(CPC + n-alkanol)/n-heptane was used [98]. In their studies both temperature and ω tendered incremental effect on the N_s. However, in the present study as we have noticed that with a fixed number of surfactant molecules, formation of larger number of droplets would reduce the average number of surfactant molecules per microemulsion droplets. This apparent unusual behavior was made possible because of the presence of oxyethylene groups in Tween-20. In Tween-20 the oxyethylene group could 'open up' or 'uncoil' itself to provide a better coverage at the oil-water interface[229]. Ionic surfactants because of their relatively smaller head groups, could not tender such effect.

It was found that both the increase in temperature and ω values led to an increase in number of droplet per unit volume and subsequent decrease in the average aggregation number of surfactants (N_s) per droplet. For a better delineation and protection of water droplets from the oil contact, the decrease in N_s needs to be compensated by an increase in the average number of cosurfactant molecule per droplet (N_{cs}). Figure 1.7B confirms such predictions in a better way. Trend in the variation of N_s and N_{cs} followed opposite path, especially while in considering their variations with ω values.

While considering the effect of alkanol chain length on the N_{cs} value it was observed that in general the N_{cs} values increased from n-butanol to n-heptanol. However N_{cs} values for n-octanol were found to lie in between n-butanol and n-pentanol. This supports the larger involvement of cosurfactant molecule in stabilizing a microemulsion droplet. n-octanol behaved more like an oil than a cosurfactant, for which its effect was different from the other cosurfactants.

Involvement of cosurfactant as surfactant substitute and their compensation effect could further be ascertained while considering the ratio of N_{cs} and $N_{s.}$ Except n-butanol, it was found that the ratio of N_{cs}/N_s increased linearly with the increase in ω value. Interestingly, the ratio was found to be independent of temperature (data not shown to save space). These results were in conformity with the earlier observations[98,223,226].

3.3. Size of the microemulsion droplets

Results on the hydrodynamic parameters of the microemulsion droplets are summarized in Table 1.7. In this table, radius of the water pool (R_w), effective radius of the microemulsion droplets (R_e), contributory effect of water pool, surfactant/cosurfactant head group and surfactant hydrocarbon tails and hydrodynamic radius during heating (R_h) and cooling (R_c) have been presented for all the systems except n-octanol (the reason stated earlier in the experimental section).

It is to be noted that R_w and R_e were obtained by computing the results of dilution measurements while the R_h and R_c were directly obtained from the dynamic light scattering measurements. Results are found to be comparable with each other. It is also to be noted that R_h values were found to be in between the R_w and R_e values. This is also not unexpected, although such reports are not available in literature. In case of water in oil microemulsion the hydrocarbon chains, being in oil continuum, do not get involved in the scattering of light. Therefore one could, in general, expect depreciation in size corresponding to the dimension (length) of the surfactant tail. According to Tanford's formula, the critical (l_c) or effective length (l_{max}) of a saturated hydrocarbon chain having C_n number of carbon atoms will be [2]:

$$l_c \leq l_{max} \approx (0.154 + 0.1265\, C_n)\ \text{nm} \qquad (1.\mathbf{27})$$

For Tween-20 (having a dodecyl hydrocarbon chain) l_c appears to be approximately equal to 1.672 nm. Therefore one could expect a difference of ≈

1.7 nm in between R_e and R_h value. For every system the radii were found to decrease with increase in temperature. Such observations, especially in the DLS measurements finally prove our assumptions as made during the analyses of dilution measurements. When the numbers of droplets are increased without changing the number of surfactant molecules, one could expect a decrease in the size of the microemulsion droplets. Also the decrease in $R_w/R_e/R_h/R_e$ values with the increase in ω values further establishes our mechanism as proposed in analyzing the results of dilution measurements. While considering the effect of cosurfactant chain length it was found that R_e values increased with the increase in cosurfactant chain length. However, no systematic variation in the radii values were evidenced through DLS measurements. Formation of larger number of droplets along with a size decreased could be further clarified through Figure 1.8.

Figure 8 describes the temperature dependence of microemulsion size and its distribution obtained from DLS measurements. It is clear from the Figure that with increase in temperature the size distribution moves to the lower dimensions. Besides, the intensity of the distribution curves was found to be increased with the rise in temperature. It is known that the light scattering intensity is proportional to the square of droplet volume and to the droplet number [232].

Table: 1.7. Radius of water/(Tween 20+ n-alkanol)/n-heptane water-in-oil microemulsion at different temperature and [water]/[Tween 20] *mole ratio, ω.*

n-alkanol		R_w / R_e / R_h / R_c (in nm) at different temperature (in K)				
	ω	Temp. 303	308	313	318	323
BuOH	5	1.34/3.20/1.85/2.19	0.96/2.52/1.54/2.00	0.80/2.23/1.34/1.88	0.78/1.94/1.38/1.65	0.65/1.90/1.40/1.40
	10	1.51/3.14/2.70/2.40	1.21/2.63/2.15/3.21	1.09/2.34/1.85/3.02	0.96/2.11/1.80/2.72	0.86/1.96/1.75/1.75
	15	1.96/3.49/3.30/2.80	1.56/2.86/2.37/2.60	1.32/2.47/2.10/1.88	1.10/2.21/2.16/1.53	0.99/2.05/2.25/2.25
	20	1.60/3.05/3.90/3.61	1.17/2.56/3.40/2.43	1.29/2.50/2.55/2.11	1.23/2.31/2.37/1.70	1.17/2.11/2.72/2.72
PentOH	5	0.96/2.93/0.91/0.80	0.93/2.66/0.81/0.86	0.78/2.46/0.74/0.84	0.70/2.33/0.78/0.83	0.66/2.20/0.86/0.86
	10	1.01/2.90/0.84/0.73	0.94/2.73/0.80/0.76	0.92/2.58/0.73/0.77	0.85/2.45/0.77/0.75	0.81/2.33/0.79/0.79
	15	0.85/2.86/0.94/0.93	0.85/2.76/0.87/0.91	0.84/2.65/0.80/0.93	0.78/2.56/0.79/0.86	0.77/2.45/0.85/0.85
	20	0.85/2.89/0.98/0.85	0.78/2.78/0.92/0.84	0.75/2.70/0.81/0.84	0.76/2.61/0.80/0.81	0.72/2.54/0.81/0.81
HexOH	5	1.17/3.23/0.75/0.49	1.23/2.96/0.65/0.50	1.07/2.73/0.60/0.51	0.96/2.63/0.52/0.55	0.92/2.40/0.55/0.55
	10	1.00/3.18/0.82/0.54	1.01/3.02/0.76/0.55	1.13/2.65/0.70/0.52	0.84/2.82/0.64/0.55	0.84/2.70/0.59/0.59
	15	0.94/3.21/0.87/0.60	0.85/3.09/0.77/0.74	0.78/3.01/0.72/0.71	0.87/2.83/0.66/0.72	0.78/2.82/0.65/0.65
	20	0.82/3.20/0.90/0.72	0.76/3.12/0.85/0.80	0.79/3.04/0.80/0.78	0.81/2.93/0.75/0.80	0.74/2.90/0.70/0.70
HeptOH	5	1.47/3.43/0.77/0.59	1.39/3.11/0.72/0.54	1.23/2.97/0.63/0.52	1.17/2.69/0.60/0.54	1.08/2.63/0.65/0.65
	10	1.04/3.52/0.95/0.65	0.99/3.40/0.83/0.62	0.94/3.26/0.72/0.65	0.92/3.12/0.67/0.65	0.89/2.98/0.64/0.64
	15	1.12/3.56/1.00/0.65	1.04/3.44/0.83/0.61	1.00/3.34/0.68/0.63	0.97/3.26/0.63/0.62	0.99/3.08/0.68/0.68
	20	1.10/3.58/0.95/0.61	1.04/3.49/0.85/0.63	1.04/3.40/0.74/0.57	1.04/3.31/0.63/0.58	1.02/3.22/0.60/0.60
OctOH	5	0.94/2.53/1.05/0.65	0.94/2.40/0.90/0.61	0.87/2.25/0.75/0.57	0.79/2.13/0.69/0.63	0.77/1.99/0.60/0.60
	10	0.77/2.46/1.15/0.76	0.74/2.38/0.90/0.68	0.75/2.30/0.81/0.69	0.72/2.21/0.71/0.65	0.70/2.13/0.68/0.68
	15	0.82/2.46/1.30/0.70	0.77/2.38/0.98/0.63	0.75/2.32/0.88/0.60	0.74/2.26/0.70/0.61	0.76/2.20/0.62/0.62
	20	0.80/2.43 /— /—	0.77/2.38 /— /—	0.80/2.33 /— /—	0.75/2.28 /— /—	0.74/2.24 /— /—

0.2 moldm^{-3} Tween 20 with 1:1 Tween 20 : n-alkanol (w/w) in n-heptane was used. R_w / R_e / R_h / R_c represent the radius of the water pool (derived from dilution measurement), effective radius of the microemulsion droplet (derived from dilution measurement), radius of droplet measured by DLS while heating and radius of droplet measured by DLS while cooling.

In the present study the increase in the number of droplets were more significant than the decrease in size of the microemulsion droplets. Hence increase in the intensity of the distribution curve was resulted along with a decrease in the width of the distribution curves. However, further structural studies on such microemulsions using cryo-transmission electron microscopy are warranted.

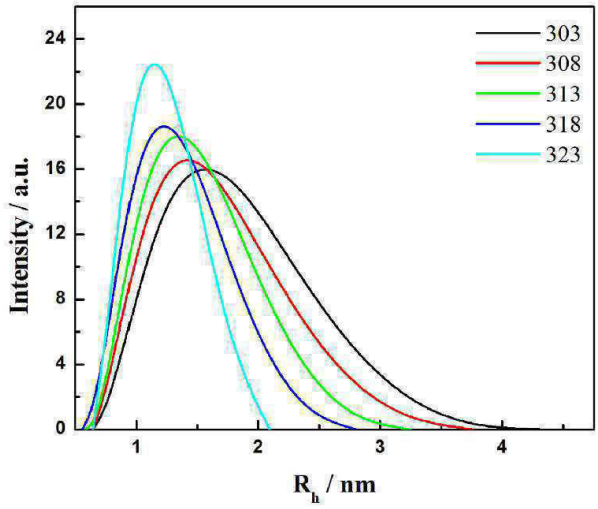

Figure 1.8. Size and size distribution of water/(Tween 20 +n-hexanol, 1:1, w/w)/n-heptane water-in-oil microemulsion at different temperatures. Temperatures (in K) have been mentioned inside the Figure [water]/[Tween 20*], ω= 10. A 0.2 moldm*$^{-3}$ Tween20 was used.

In recording the DLS data while cooling down microemulsions, it was always noted that dimensions of the droplets to follow a higher profile than the heating curves. This unusual behavior was due to the condensation effect of the droplets during the cooling [232]. However, the width of the distribution curves were not changed significantly as what was observed during the heating of the microemulsions.

3.4. Viscosity measurement

Viscosity along with viscosity derived activation parameters at 1:1 Tween20-alkanol ratio under different conditions have been summarized in Table 4. η and temperature dependency of data have been presented in Figure 1.9 for n-hexanol derived formulation as representative plot. It was generally observed that

with the rise in temperature viscosity decreased. Viscosity initially decreases with increasing ω and passes through minima at ω in the range of 10 to 15. It is known that fluidity increases with the rise in temperature for microemulsions in general[114,127,128]. However, initial decrease in viscosity of microemulsion with increase in ω could be accounted for the increase in number of droplets, and subsequent size depletion. Viscosity was found to increase with the increase in cosurfactant chain length. This is due to the stronger binding affinity of alkanol with surfactant head groups[223]. However n-octanol being more oily than other cosurfactants did not tender progressive incremental effect. Temperature dependency of viscosity was found to decrease with the increase in cosurfactant chain length. Further investigations using more sophisticated tools like small angle neutron scattering and cryo-TEM, etc., are warranted. Therefore, rheometric measurements, along with above mentioned studies on such systems could be considered as the future perspectives of the present work.

As expressed in equation (29); one can obtain ΔH^* from the slope of ln η vs T^{-1} plot. ln η was found to vary with T^{-1} in a binomial way; hence one can derive ΔH^* from it's differential with respect to temperature in the following way;

$$\ln \eta = a + bT + cT^2 \qquad \textbf{(1.30)}$$

Therefore,

$$\frac{d ln \eta}{dT} = -\frac{\Delta H^*}{RT^2} = b + 2cT \qquad \textbf{(1.31)}$$

Thus knowing the value of 'b' and 'c' one can compute ΔH^* at different temperatures.

Change in heat capacity (ΔC_p) is related to ΔH^* as;

$$\Delta C_p = \frac{d(\Delta H^*)}{dT} = -2RT(b + 3cT) \qquad \textbf{(1.32)}$$

Table: 1.8. Viscosity and viscosity derived activation parameters of water/(Tween 20+n-alkanol)/n-heptane water-in-oil microemulsion at different temperatures and [water]/[Tween 20*] mole ratio, ω.*

n-alkanol		$(\eta/cP) / \Delta H^*/kJmol^{-1}) / (\Delta G^*/kJmol^{-1}) / (\Delta S^* / J\ mol^{-1}K^{-1}) / (\Delta C_p/ kJ\ mol^{-1}K^{-1})$				
	ω	303	308	313	318	323
BuOH	5	2.88/7.17/3.52/2.36/7.10	2.56/7.53/3.54/2.44/7.33	2.34/7.90/3.58/2.52/7.58	1.80/8.30/3.57/2.60/7.82	1.34/8.68/3.55/2.69/8.07
	10	2.66/8.30/3.50/2.73/8.21	2.45/8.72/3.53/2.83/8.49	2.10/9.14/3.55/2.92/8.76	1.56/9.59/3.53/3.01/9.05	1.14/10.05/3.50/3.11/9.33
	15	2.80/5.60/3.51/1.85/5.54	2.39/5.88/3.53/1.91/5.73	1.91/6.17/3.53/1.97/5.92	1.34/6.47/3.49/2.03/6.10	1.01/6.78/3.48/2.10/6.30
	20	2.77/8.34/3.51/2.91/8.75	2.37/9.28/3.53/3.01/9.04	2.15/9.74/3.56/3.11/9.33	1.70/10.22/3.55/3.21/9.64	1.12/10.70/3.50/3.31/9.94
	5	2.80/6.73/3.51/2.22/6.66	2.58/7.07/3.55/2.29/6.88	2.44/7.42/3.59/2.37/7.11	1.86/7.78/3.58/2.44/7.34	1.49/8.15/3.58/2.52/7.57
	10	2.90/2.28/3.52/0.75/2.26	2.38/2.39/3.53/0.78/2.33	2.38/2.51/3.58/0.80/2.41	1.86/2.63/3.58/0.83/2.50	1.60/2.77/3.60/0.85/2.60
	15	2.84/1.61/3.52/0.53/1.59	2.50/1.69/3.54/0.54/1.64	2.32/1.77/3.59/0.56/1.70	1.96/1.86/3.59/0.58/1.76	1.72/1.95/3.61/0.60/1.81
	20	2.96/3.44/3.53/1.13/3.41	2.68/3.62/3.56/1.18/3.53	2.50/3.80/3.60/1.21/3.64	2.20/3.98/3.62/1.25/3.75	1.81/4.17/3.63/1.29/3.88
	5	3.17/1.03/3.54/0.34/1.02	3.01/1.09/3.59/0.35/1.05	2.81/1.13/3.63/0.36/1.09	2.60/1.19/3.67/0.37/1.12	2.40/1.25/3.70/0.39/1.16
	10	3.09/-4.40/3.53/-1.45/-4.36	2.80/-4.62/3.57/-1.50/-4.50	2.47/-4.86/3.60/-1.55/-4.65	2.30/-5.09/3.63/-1.60/-4.80	2.44/-5.33/3.71/-1.69/-4.95
	15	3.15/2.97/3.54/9.81/2.94	2.89/3.12/3.58/1.01/3.04	2.60/3.27/3.61/1.04/3.14	2.39/3.43/3.64/1.08/3.24	1.95/3.60/3.65/1.11/3.34
	20	3.30/3.00/3.55/0.99/2.98	2.90/3.15/3.58/1.02/3.07	2.70/3.31/3.62/1.05/3.18	2.27/3.47/3.63/1.09/3.28	1.89/3.64/3.64/1.12/3.38
	5	3.59/1.98/3.58/0.65/1.96	3.20/2.07/3.60/0.67/2.02	3.05/2.17/3.65/0.69/2.08	2.72/2.28/3.68/0.72/2.16	2.34/2.39/3.70/0.74/2.22
	10	3.23/0.29/3.54/0.09/0.29	2.95/0.31/3.59/0.01/0.30	2.73/0.32/3.62/0.01/0.31	2.55/0.34/3.66/0.10/0.32	2.31/0.36/3.69/0.11/0.33
	15	3.24/5.98/3.55/1.97/5.92	3.13/6.28/3.60/2.04/6.12	3.32/6.59/3.68/2.10/6.32	2.80/6.91/3.69/2.17/6.52	2.41/7.25/3.71/2.24/6.73
	20	3.54/0.55/3.73/0.18/0.54	3.31/0.58/3.61/0.18/0.56	3.04/0.60/3.65/0.19/0.58	2.82/0.63/3.69/0.20/0.60	2.59/0.67/3.72/0.20/0.62
OctOH	5	3.44/-0.80/3.56/-0.26/-0.80	3.16/-0.84/3.60/-0.27/-0.85	2.95/-0.89/3.64/-0.28/-0.85	2.68/-0.93/3.67/-0.29/-0.88	2.60/-0.98/3.73/-0.30/-0.90
	10	3.47/0.58/3.60/0.19/0.58	3.18/0.61/3.60/0.20/0.62	2.99/0.64/3.65/0.20/0.62	2.75/0.68/3.68/0.21/0.64	2.51/0.71/3.72/0.22/0.66
	15	3.60/-0.68/3.57/-0.22/-0.67	3.41/-0.71/3.62/-0.23/-0.72	3.09/-0.75/3.65/-0.24/-0.72	3.19/-0.78/3.72/-0.25/-0.74	2.92/-0.82/3.76/-0.26/-0.76

0.2 moldm^{-3} Tween 20 with 1:1 Tween 20: n-alkanol (w/w) in n-heptane was used. η: viscosity; ΔH^*: Enthalpy change; ΔG^*: free energy change; ΔS^*:entropy change and ΔC_p: heat capacity change.

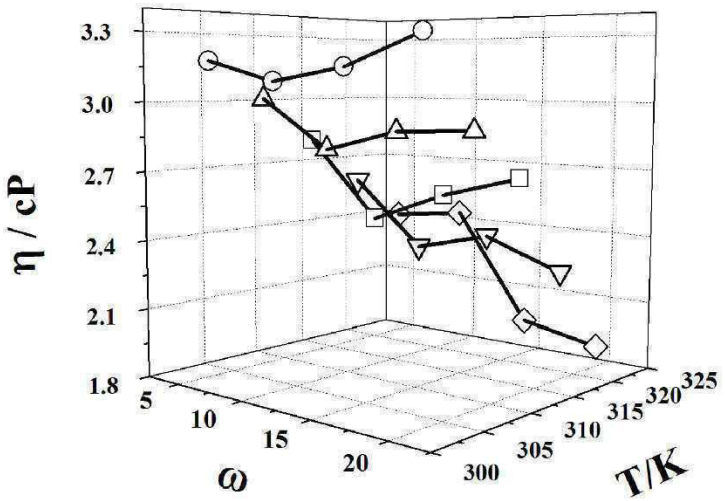

Figure 1.9. *Viscosity (η) – ω –* T profile for the microemulsion comprising of water/ (Tween 20 +n-hexanol)/n-heptane. 0.2 moldm^{-3} Tween 20 with a 1:1 (w/w) ratio of n-hexanol was used.

Therefore change in Gibb's free energy for activation could be expressed as;

$$\Delta G^* - RT\ ln\frac{\eta V}{hN} \qquad (1.\mathbf{33})$$

Once ΔH^* and ΔG^* are known, the ΔS^* value could be calculated easily according to the following expression:

$$\Delta S^* = \frac{\Delta H^* - \Delta G^*}{T} \qquad (1.\mathbf{34})$$

All the viscosity associated thermodynamic parameters have been presented in Table 1.4. The results reveal that ω dependency on ΔG^* was almost similar like its viscosity. Gibb's free energy for activation was found to increase with temperature for all the systems. The increase in ΔG^* with temperature is a consequence of shear thickening of the sample with increasing temperature. No systematic variations in the ΔC_p values were noted. Both the positive and negative ΔC_p values were in accordance with increase and decrease in ΔH^* values under various conditions[233,234]. Results also reveal the complex nature of the microemulsion droplets. The ΔG^* values were limited within the range of 3.5 to 3.8 kJ mol^{-1} whereas the ΔH^* and ΔS^* values varied significantly. Good correlation between ΔH^* and ΔS^* were found for all the compositions and

temperature as revealed from the compensation plots between ΔH^* and ΔS^* (given in Figure 10).

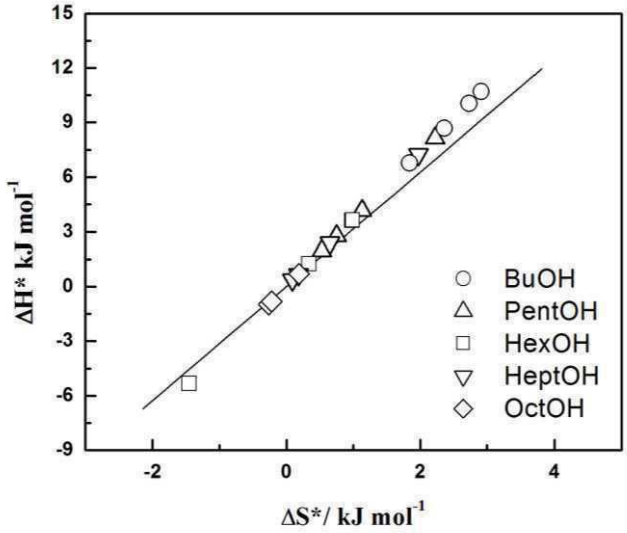

Figure 1.10. Viscosity derived activation enthalpy-entropy compensation plot for water/(Tween 20+n-alkanol)/n-heptane water-in-*oil microemulsion. All the ω values at* different experimental temperatures were considered. n-alkanols used have been mentioned inside the figure. Compensation temperatures: 313K (close to the average of the experimental temperature range 303-323K, i.e., 313K).

The compensation temperature (313K) obtained from the slope was found to be in close proximity with the average of all experimental temperatures (303, 308, 313, 318 and 323 K). Similar observations have also been reported by others[114,127,128].

4. Summary and conclusion

Physico-chemical studies on water/(Tween 20+n-alkanol)/n-heptane microemulsions were performed using different techniques, viz., phase manifestation, dilution method, DLS and viscosity measurements. Results were analyzed in the light of the above mentioned experiments. Based on the observations, the following conclusions could be made:

(1) The clarity of microemulsion formulation was reduced with the increase in cosurfactant chain length with an optimum efficacy tendered by n-hexanol.

(2) While the surfactants reside at the oil-water interface, the cosurfactants were partitioned in between the oil and oil-water interface.

(3) Spontaneity of microemulsion formation increased with increase in cosurfactant chain length, increase in temperature and decrease in the volume of the dispersed phase, water.

(4) The formation of microemulsion was found to be an enthalpy controlled process.

(5) Larger numbers of droplets were formed at the expense of size. With the increase in temperature and ω value, size reduction was also evidenced by DLS measurements.

(6) Depletion in the aggregation number of surfactant per droplet was compensated by the cosurfactant molecules. However, the compensatory effect was not affected by temperature.

(7) A symmetric variation in different physico-chemical properties were noted with the increase in the cosurfactant chain length. However, n-octanol, being oilier in nature than a cosurfactant, tendered different behavior.